nature photonics

LETTERS

PUBLISHED ONLINE: 7 MARCH 2016 | DOI: 10.1038/NPHOTON.2016.21

Electrically pumped continuous-wave III–V quantum dot lasers on silicon

Siming Chen[1]*, Wei Li[2], Jiang Wu[1], Qi Jiang[1], Mingchu Tang[1], Samuel Shutts[3], Stella N. Elliott[3], Angela Sobiesierski[3], Alwyn J. Seeds[1], Ian Ross[2], Peter M. Smowton[3] and Huiyun Liu[1]*

Reliable, efficient electrically pumped silicon-based lasers would enable full integration of photonic and electronic circuits, but have previously only been realized by wafer bonding. Here, we demonstrate continuous-wave InAs/GaAs quantum dot lasers directly grown on silicon substrates with a low threshold current density of 62.5 A cm^{-2}, a room-temperature output power exceeding 105 mW and operation up to 120 °C. Over 3,100 h of continuous-wave operating data have been collected, giving an extrapolated mean time to failure of over 100,158 h. The realization of high-performance quantum dot lasers on silicon is due to the achievement of a low density of threading dislocations on the order of 10^5 cm^{-2} in the III–V epilayers by combining a nucleation layer and dislocation filter layers with *in situ* thermal annealing. These results are a major advance towards reliable and cost-effective silicon-based photonic–electronic integration.

Increased data throughput between silicon processors in modern information processing requires unprecedented bandwidth and low power consumption beyond the capability of conventional copper interconnects. To meet these requirements, silicon photonics has been under intensive study in recent years[1,2]. Despite rapid progress being made in silicon-based light modulation and detection technology and low-cost silicon optoelectronic integrated devices enabled by the mature CMOS technology[3,4], an efficient, reliable and electrically pumped laser on a silicon substrate has remained an unrealized scientific challenge[5]. Group IV semiconductors such as silicon and germanium, widely used in integrated circuits, are inefficient light-emitting materials due to their indirect bandgap, a fact that has been a major barrier to the development of silicon photonics. Integration of III–V materials on a silicon platform has been one of the most promising techniques for generating coherent light on silicon. III–V semiconductors with superior optical properties, acting as optical gain media, can either be bonded to or epitaxially grown on silicon substrates[6–11], with the latter approach being more attractive for large-scale, low-cost and streamlined fabrication. However, until now, material lattice mismatch and incompatible thermal expansion coefficients between III–V materials and silicon substrates have fundamentally limited the monolithic growth of III–V lasers on silicon substrates by introducing high-density threading dislocations (TDs)[12].

Lasers with active regions formed from III–V quantum dots (QDs)—nanosized crystals—can not only offer low threshold current density (J_{th}), but can also provide reduced temperature sensitivity[13–17]. As shown in Fig. 1a, in a period of less than ten years the performance (in terms of J_{th}) of QD lasers has surpassed that of state-of-the-art quantum-well (QW) lasers, which have been under development over the last few decades. QD lasers have now been demonstrated with nearly constant J_{th}, output power (P_{out}) and slope efficiency at operating temperatures of up to 100 °C (ref. 18). Very recently, III–V QD structures have drawn increasing attention for the implementation of compound semiconductor lasers on silicon substrates[8–10,19]. This is because QDs have also been proved to be less sensitive to defects than conventional bulk materials and QW structures, due to carrier localization and hence reduced interaction with the defects[20]. As shown in Fig. 1b,c, a TD can only 'kill' a very limited number of QDs, leaving the rest intact and able to provide optical gain. The enhanced tolerance to defects by localized states has also been witnessed in defect-insensitive nitride semiconductors, which are now used for the most efficient lighting technology[21]. More importantly, Fig. 1b,c also shows that the TD can be either pinned or propelled away from QDs. Therefore, the strong strain field of a QD array also prevents the in-plane motion of dislocations and therefore superior reliability is expected from QD lasers compared with QW or bulk devices, even in the presence of high-density dislocations[22,23].

These unique properties of QDs provide a promising route towards monolithic III–V-on-silicon (III–V/Si) integration. As shown in Fig. 1a, III–V QD lasers grown on silicon are rapidly approaching the performance of those grown on native GaAs substrates[24,25]. In addition, high-performance QD lasers have been successfully demonstrated on Ge-on-Si and germanium substrates, offering an, albeit indirect, route to III–V/Si integration[9,10,26]. However, it would be more attractive to realize a laser that did not require the intermediate germanium layer, both because the requirement for the germanium layer restricts the range of silicon circuits to which it can be applied and because it is difficult to couple light through this layer to a silicon waveguide due to the large optical absorption coefficient of germanium at telecommunications wavelengths. Therefore, a high-performance III–V laser directly grown on a silicon substrate is the preferred solution for silicon photonic–electronic integration.

Although QD lasers have demonstrated superior performance on silicon substrates in the last few years, our previous publications[8,24,25] indicate that epitaxially grown GaAs-on-Si substrates are much inferior when compared to native GaAs substrates in terms of total defect density, typically over 2×10^6 cm^{-2} compared with $\sim 1 \times 10^3$ to 1×10^4 cm^{-2} for a GaAs substrate[27]. Furthermore, a high-performance electrically pumped continuous-wave (c.w.) QD laser directly grown on a silicon substrate has not yet been demonstrated. Here, by developing high-quality GaAs films with low TD density in the range of 10^5 cm^{-2}, we demonstrate experimentally high-performance 1,310 nm InAs/GaAs QD lasers directly grown on silicon, with a record low J_{th}, high power and high-temperature c.w. operation. Most significantly, a large number of operating hours with negligible degradation has been demonstrated for III–V lasers directly grown on silicon substrates.

[1]Department of Electronic and Electrical Engineering, University College London, London WC1E 7JE, UK. [2]Department of Electronic and Electrical Engineering, University of Sheffield, Sheffield S1 3JD, UK. [3]Department of Physics and Astronomy, Cardiff University, Queens Building, The Parade, Cardiff CF24 3AA, UK. *e-mail: siming.chen@ucl.ac.uk; huiyun.liu@ucl.ac.uk

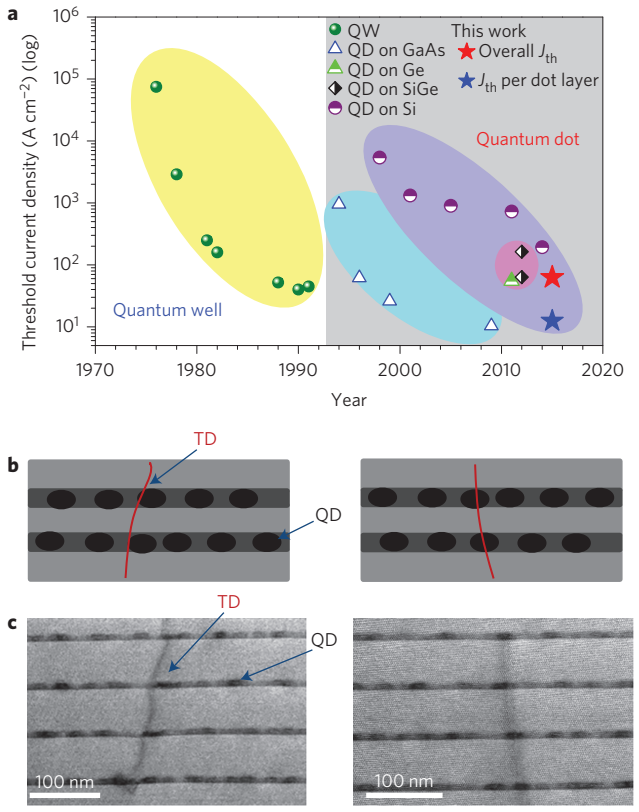

Figure 1 | Development and advantages of QD lasers. a, The historical development of low-dimensional heterostructure lasers, showing the record threshold current densities. The red star indicates the threshold value achieved in this work. The blue star is the value normalized to a single QD layer. **b**, Schematic of the interaction between QDs and threading dislocations. **c**, Bright-field scanning TEM images showing the potential interactions between threading dislocations and QDs.

In this work, InAs/GaAs QD lasers were directly grown on silicon substrates using a solid-source molecular beam epitaxy (MBE) system. To realize high-quality III–V lasers on silicon, it is necessary to minimize the impact of dislocations. Otherwise, TDs propagating into the active region will form non-radiative recombination centres and reduce minority-carrier lifetimes[23], leading to degradation of laser performance. To realize practical monolithic QD lasers with the performance and reliability required for monolithic integration, several strategies have been developed and employed in the present work. First, to prevent the formation of antiphase domains (APDs) while growing polar III–V materials on nonpolar silicon substrates, phosphorus-doped Si(100) wafers with 4° offcut to the [011] plane were used[28] (Supplementary Fig. 1 and Supplementary Section I). A thin nucleation layer made of AlAs was deposited by migration enhanced epitaxy using alternating Al and As_4 flux at a low growth temperature of 350 °C. Figure 2a presents a high-angle annular dark-field scanning transmission electron microscopy (TEM) image of the interface. The thin AlAs nucleation layer has suppressed three-dimensional growth and provides a good interface for succeeding III–V material growth[19]. Following the AlAs nucleation layer, a three-step growth technique of GaAs epitaxial growth was performed[8,29]. The three layers of GaAs were grown at 350, 450 and 590 °C for 30, 170 and 800 nm, respectively. As shown in Fig. 2b, most of the defects are well confined in the first 200 nm region thanks to the nucleation layer and multistep temperature growth, but a high density (1×10^9 cm^{-2}) of TDs are still seen to propagate towards the active region. To further improve the material quality, strained-layer superlattices (SLSs) were grown as dislocation filter layers (DFLs) on the top of the GaAs buffer layer. Each SLS is made of five periods of 10 nm $In_{0.18}Ga_{0.82}As$/10 nm GaAs, which are repeated four times, separated by 300 nm GaAs spacing layers. The strain relaxation of the SLSs applies an in-plane force to the TDs, which enhances the lateral motion of TDs considerably, and hence increases the probability of annihilation. *In situ* thermal annealing of the SLS was also carried out four times, with the growth paused in the MBE reactor by increasing the substrate temperature to 660 °C for 6 min. This approach can further improve the efficacy of filtering defects by increasing the mobility of the defects, leading to their annihilation before growth of the subsequent layers. As shown in Fig. 2b,c, each set of $In_{0.18}Ga_{0.82}As$/GaAs SLSs can reduce the dislocation density by a few times. After the 300 nm GaAs spacer layers of the last SLSs, the dislocation density is reduced to the order of 10^5 cm^{-2}, beyond the reliable measurement capability of cross-sectional TEM images. A typical atomic force microscopy (AFM) image for an uncapped QD sample grown on a silicon substrate with exactly the same conditions is shown in the inset of Fig. 2d. A good QD uniformity is obtained with a density of $\sim 3.0 \times 10^{10}$ cm^{-2}. Based on the developed template, a standard five-layer QD laser structure was then grown. A room-temperature photoluminescence emission at ~1,300 nm with a full-width at half-maximum (FWHM) of ~29 meV was obtained, as shown in the Fig. 2d, indicating a relatively small dot inhomogeneity. More uniformity studies of QDs grown on Si are presented in Supplementary Fig. 3 (Supplementary Section II). Cross-sectional scanning TEM measurements were used to characterize the QD active region grown on silicon substrates. The typical dot size is ~20 nm in diameter and ~7 nm in height, as shown in Fig. 2e (top left). The high-resolution high-angle annular dark-field scanning TEM images of a single dot also, to a large extent, show a uniform indium distribution with marginal intermixing, as shown in Fig. 2e (bottom left). In addition, a nearly defect-free dot-in-well (DWELL) active region is observed, as shown in Fig. 2e (right) and Supplementary Fig. 2 (Supplementary Section I).

Broad-area lasers were fabricated as shown schematically in Fig. 3a. The lasers were processed with as-cleaved facets. A cross-sectional scanning electron microscope (SEM) image of a fabricated InAs/GaAs QD laser on a silicon substrate is shown in Fig. 3b. It can be seen that a very clean and mirror-like facet has been achieved. This is important, because imperfectly cleaved facets result in increased mirror loss and reduced differential external quantum efficiency. No coatings were applied to the facets. An SEM overview of a complete III–V laser on silicon is shown in Fig. 3c. Laser bars were then mounted on gold-plated copper heatsinks using indium–silver low-melting-point solder and gold-wire-bonded to enable testing (Supplementary Section III).

Low J_{th} and high optical P_{out} are always desirable goals for laser applications. Figure 4a shows the light–current–voltage (LIV) measurements for an InAs/GaAs QD laser grown on a silicon substrate under c.w. operation at room temperature. A clear knee behaviour in the LI curve is observed at the lasing J_{th} of 62.5 A cm^{-2}, which corresponds to 12.5 A cm^{-2} for each of the five QD layers. To the best of our knowledge, this value of J_{th} represents the lowest c.w. room-temperature J_{th} for any kind of laser on a silicon substrate to date and is comparable to the best-reported values for conventional QD lasers on a GaAs substrate[13,30]. The P_{out} measured from both facets is as high as 105 mW at an injection current density of 650 A cm^{-2}, with no evidence of power saturation up to this current density.

In many cases, the lasers exhibit nonlinearity or 'kinks' in the above-threshold LI characteristics. To understand the origin of this behaviour, the evolution of emission spectra at various c.w. injection current densities is presented in Fig. 4b. At a low injection of 50 A cm^{-2}, a broad spontaneous emission with a FWHM of 38 nm is observed at a peak wavelength of 1,316 nm. As the current density increases to 62.5 A cm^{-2}, the peak at 1,315 nm increases

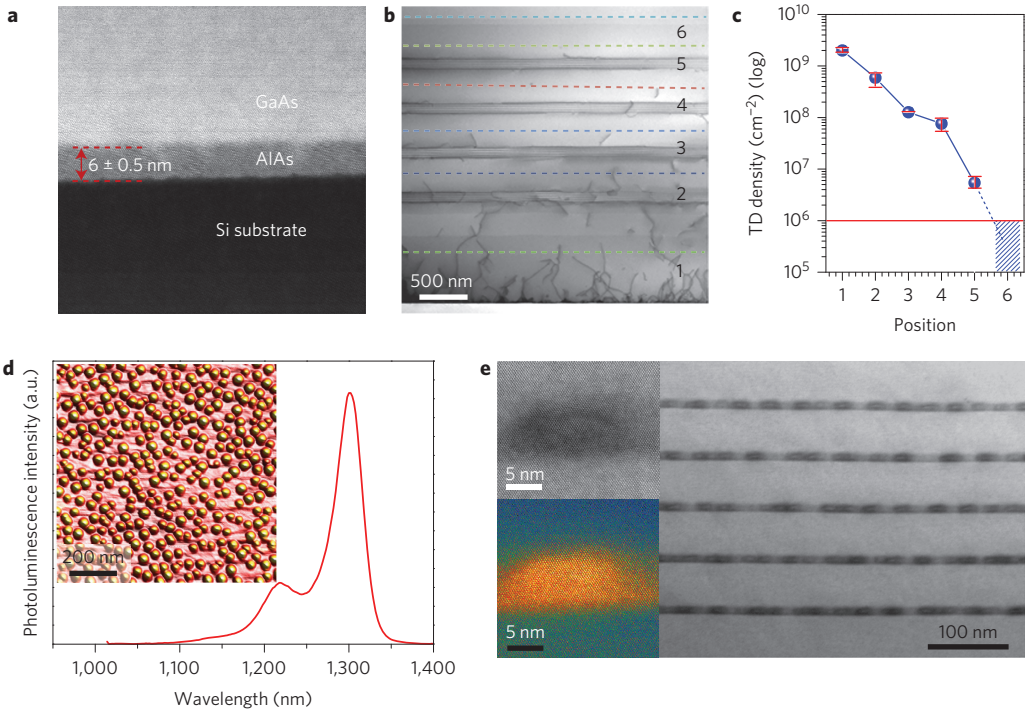

Figure 2 | Epitaxial growth and structural characterization of QD lasers. a, High-angle annular dark-field scanning TEM image of the interface between the 6 nm AlAs nucleation layer and a silicon substrate. **b**, Bright-field scanning TEM image of DFLs. **c**, Dislocation density measured at different positions, as indicated in **b**. **d**, Photoluminescence spectrum for a QD active region grown on silicon. Inset: representative AFM image of an uncapped QD sample grown on silicon. **e**, High-resolution bright-field scanning TEM images of a single dot (top left), corrected high-angle annular dark-field scanning TEM images (false colour) of a single QD (bottom left) and bright-field scanning TEM image of the QD active layers (right).

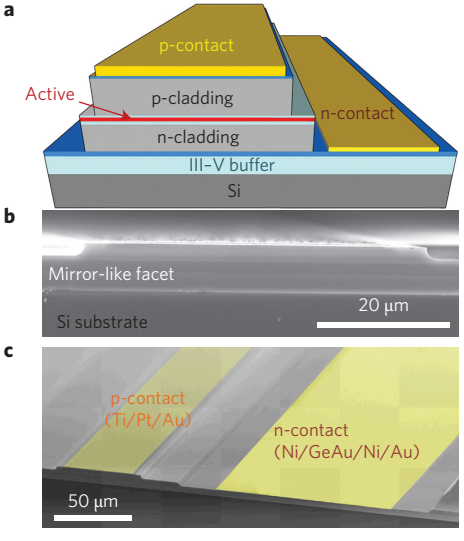

Figure 3 | Fabricated III–V laser directly grown on a silicon substrate. **a**, Schematic of the layer structure of an InAs/GaAs QD laser on a silicon substrate. **b**, A cross-sectional SEM image of the fabricated laser with as-cleaved facets, showing very good facet quality. **c**, SEM overview of the complete III–V laser on silicon.

sharply in intensity and narrows to 2.4 nm, which is obvious evidence of lasing. Further increasing the injection current density gives rise to multimode lasing, which becomes more pronounced at increasingly higher injection levels. Lasing operation from the excited states is not observed up to the maximum injection of 650 A cm^{-2}, which indicates that those kinks observed in the LI curve are mainly related to mode competition and carrier redistributions between different modes within the ground state. This behaviour is characteristic of broad-area laser structures, and the nonlinear effects are also observed in the near-field of the laser, which evolves with carrier injection (Supplementary Section IV).

In addition to J_{th} and P_{out}, for silicon photonic–electronic integration applications, it is important that lasers can operate at high temperature in c.w. mode. This is required because silicon-based electronic chips are often required to work in ambient temperatures of 65 °C or even higher, without the use of thermo-electric cooling. Figure 4c shows the c.w. P_{out} for the QD laser at various temperatures. The c.w. lasing in the ground state was maintained until the testing was stopped at a heatsink temperature of 75 °C due to the limitation of the c.w. current source. This silicon-based laser has also been tested under pulsed operation, and lasing up to 120 °C was demonstrated with limited self-heating (Supplementary Section IV). To the best of our knowledge, this is the first demonstration of QD lasers directly grown on silicon substrates that lase up to 75 and 120 °C under c.w. and pulsed operation, respectively. The characteristic temperature T_0 for this device as estimated under pulsed operation is 51 K between 20 and 60 °C and 35 K between 70 and 120 °C (Supplementary Section IV).

A critical requirement for the practical application of electrically pumped lasers on silicon is to achieve sufficient operating lifetime. High reliability, in terms of a long mean time to failure (MTTF) is an important prerequisite to establish the feasibility of delivering commercial III–V QD lasers directly grown on silicon substrates. Here, we present the results from our lifetime study on the InAs/GaAs QD laser epitaxially grown directly on a silicon substrate. The ageing test was performed at a fixed temperature of 26 °C, with the P_{out} monitored for a constant c.w. drive current of 210 mA, which corresponds to 1.75 times the threshold current. Periodic LIV characterizations were also performed to monitor changes in the lasing threshold. The ageing results are shown in Fig. 4d. A 29.7%

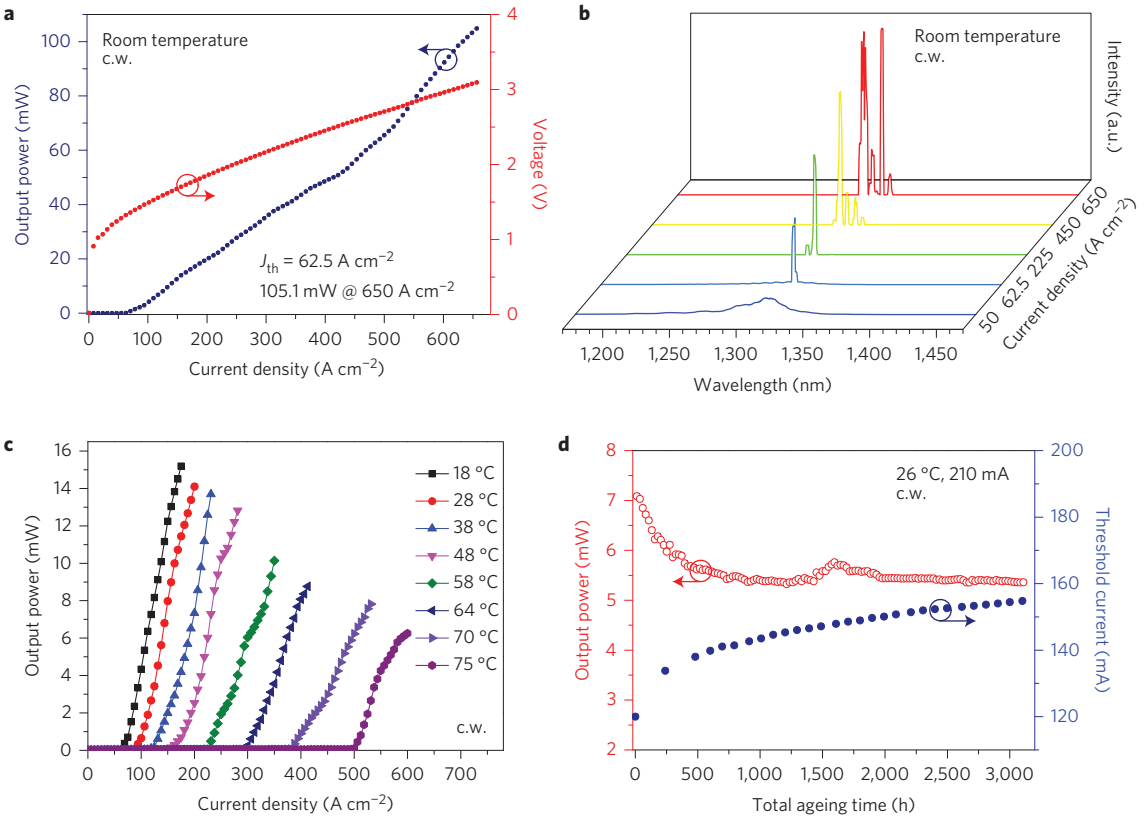

Figure 4 | Silicon laser performance characterization. a, LIV characteristics for a 50 μm × 3,200 μm InAs/GaAs QD laser grown on a silicon substrate under c.w. operation at 18 °C. **b**, Emission spectra for a 50 μm × 3,200 μm InAs/GaAs QD laser grown on a silicon substrate at various injection current densities under c.w. operation at 18 °C. **c**, Light output power versus current density for this InAs/GaAs QD laser on silicon at various heatsink temperatures. **d**, Ageing data for the InAs/GaAs QD laser on silicon at a constant heatsink temperature of 26 °C and c.w. drive current of 210 mA.

drop in power over the ageing test period of 3,100 h is observed, with most of the drop (26.4%) occurring in the first 500 h, followed by a very slow degradation of light output over time. A similar trend was observed for the threshold behaviour, where most of the increase in threshold occurred in the early stages of testing. An extrapolated MTTF (defined by a doubling of the threshold) of over 100,158 h was determined from fitting the threshold with a sublinear model (Supplementary Section V)[23]. It should be noted that these data represent the worst case results, because (1) the laser was operated epitaxial side up, (2) the laser was not hard soldered to a high-thermal-conductivity heatsink, and (3) no facet coatings were used. Nevertheless, the estimated lifetime is much longer than the best reported extrapolated MTTF of 4,627 h for a p-doped InAs/GaAs QD laser grown on a Ge-on-Si 'virtual' substrate[23]. If the standard industrial techniques described above were to be used, an even better lifetime performance would be expected.

The realization of high-quality GaAs-on-silicon layers with low defects by applying the combined strategies of an AlAs nucleation layer, InGaAs/GaAs DFLs, *in situ* thermal annealing and using QDs as laser active regions (developed using the MBE epitaxial growth method) represents a major step towards substituting III–V/Si epitaxy for the III–V on Ge and Ge-on-Si 'virtual' substrates. Our results demonstrate that the large lattice mismatch between III–V materials and silicon will no longer be a fundamental hurdle for monolithic epitaxial growth of III–V photonic devices on silicon substrates. In particular, we have achieved c.w. lasing up to 75 °C, with an ultralow c.w. J_{th} of 62.5 A cm^{-2}, a high output power exceeding 105 mW at room temperature, and a long extrapolated lifetime of over 100,158 h. Our demonstration of the ability to grow uniform high-quality III–V materials over the whole silicon substrate and then fabricate electrically pumped lasers operating in c.w. mode to high temperature, with high uniformity and long lifetime, opens up new possibilities for silicon photonics and for the direct integration of optical interconnects on the silicon-based microelectronics platform.

Methods

Methods and any associated references are available in the online version of the paper.

Received 8 November 2015; accepted 25 January 2016; published online 7 March 2016

References

1. Asghari, M. & Krishnamoorthy, A. V. Silicon photonics: energy-efficient communication. *Nature Photon.* **5,** 268–270 (2011).
2. Rickman, A. The commercialization of silicon photonics. *Nature Photon.* **8,** 579–582 (2014).
3. Virot, L. *et al.* Germanium avalanche receiver for low power interconnects. *Nature Commun.* **5,** 4957 (2014).
4. Reed, G. T., Mashanovich, G., Gardes, F. & Thomson, D. Silicon optical modulators. *Nature Photon.* **4,** 518–526 (2010).
5. Camacho-Aguilera, R. E. *et al.* An electrically pumped germanium laser. *Opt. Express* **20,** 11316–11320 (2012).
6. Tanabe, K., Watanabe, K. & Arakawa, Y. III–V/Si hybrid photonic devices by direct fusion bonding. *Sci. Rep.* **2,** 349 (2012).
7. Mi, Z., Yang, J., Bhattacharya, P. & Huffaker, D. Self-organised quantum dots as dislocation filters: the case of GaAs-based lasers on silicon. *Electron. Lett.* **42,** 121–123 (2006).
8. Wang, T., Liu, H., Lee, A., Pozzi, F. & Seeds, A. 1.3-μm InAs/GaAs quantum-dot lasers monolithically grown on Si substrates. *Opt. Express* **19,** 11381–11386 (2011).
9. Lee, A., Jiang, Q., Tang, M., Seeds, A. & Liu, H. Continuous-wave InAs/GaAs quantum-dot laser diodes monolithically grown on Si substrate with low threshold current densities. *Opt. Express.* **20,** 22181–22187 (2012).
10. Liu, A. *et al.* High performance continuous wave 1.3 μm quantum dot lasers on silicon. *Appl. Phys. Lett.* **104,** 041104 (2014).

11. Wang, Z. *et al.* Room-temperature, InP distributed feedback laser array directly grown on silicon. *Nature Photon.* **9,** 837–842 (2015).
12. Zhou, Z. *et al.* On-chip light sources for silicon photonics. *Light Sci. Appl.* **4,** e358 (2015).
13. Deppe, D., Shavritranuruk, K., Ozgur, G., Chen, H. & Freisem, S. Quantum dot laser diode with low threshold and low internal loss. *Electron. Lett.* **45,** 54–56 (2009).
14. Arakawa, Y. *et al.* Multidimensional quantum well laser and temperature dependence of its threshold current. *Appl. Phys. Lett.* **40,** 939–941 (1982).
15. Crowley, M. T., Naderi, N. A., Su, H., Grillot, F. & Lester, L. F. GaAs-based quantum dot lasers. *Semiconductors Semimetals* **86,** 371–417 (2012).
16. Bimberg, D. *et al. Quantum Dot Heterostructures* (Wiley, 1999).
17. Liu, G. T. *et al.* Extremely low room-temperature threshold current density diode lasers using InAs dots in $In_{0.15}Ga_{0.85}As$ quantum well. *Electron. Lett.* **35,** 1163–1165 (1999).
18. Sugawara, M. & Usami, M. Quantum dot devices: handling the heat. *Nature Photon.* **3,** 30–31 (2009).
19. Lee, A. D. *et al.* InAs/GaAs quantum-dot lasers monolithically grown on Si, Ge, and Ge-on-Si substrates. *IEEE J. Sel. Top. Quantum Electron.* **19,** 1901107 (2013).
20. Mi, Z. *et al.* High-performance quantum dot lasers and integrated optoelectronics on Si. *Proc. IEEE* **97,** 1239–1248 (2009).
21. Chichibu, S. F. *et al.* Origin of defect-insensitive emission probability in In-containing (Al, In, Ga) N alloy semiconductors. *Nature Mater.* **5,** 810–816 (2006).
22. Beanland, R. *et al.* Structural analysis of life tested 1.3 μm quantum dot lasers. *J. Appl. Phys.* **103,** 014913 (2008).
23. Liu, A. *et al.* Reliability of InAs/GaAs quantum dot lasers epitaxially grown on silicon. *IEEE J. Sel. Top. Quantum Electron.* **21,** 1900708 (2015).
24. Tang, M. *et al.* 1.3-μm InAs/GaAs quantum-dot lasers monolithically grown on Si substrates using InAlAs/GaAs dislocation filter layers. *Opt. Express* **22,** 11528–11535 (2014).
25. Chen, S. *et al.* 1.3 μm InAs/GaAs quantum-dot laser monolithically grown on Si substrates operating over 100 °C. *Electron. Lett.* **50,** 1467–1468 (2014).
26. Liu, H. *et al.* Long-wavelength InAs/GaAs quantum-dot laser diode monolithically grown on Ge substrate. *Nature Photon.* **5,** 416–419 (2011).
27. Tischler, M. A. *et al.* Defect reduction in GaAs epitaxial layer using a GaAsP–InGaAs strained-layer superlattice. *Appl. Phys. Lett.* **46,** 294–296 (1985).
28. Fischer, R. *et al.* Dislocation reduction in epitaxial GaAs on Si(100). *Appl. Phys. Lett.* **48,** 1223–1225 (1986).
29. Akiyama, M. *et al.* Growth of single domain GaAs layer on (100)-oriented Si substrate by MOCVD. *Jpn J. Appl. Phys.* **23,** L843 (1984).
30. Sellers, I. *et al.* 1.3 μm InAs/GaAs multilayer quantum-dot laser with extremely low room-temperature threshold current density. *Electron. Lett.* **40,** 1412–1413 (2004).

Acknowledgements

The authors acknowledge financial support from the UK Engineering and Physical Sciences Research Council (grants nos. EP/J012904/1 and EP/J012815/1). H.L. thanks The Royal Society for funding his University Research Fellowship.

Author contributions

H.L. proposed and guided the overall project with contributions from A.J.S. and P.M.S. S.C., J.W., A.J.S., P.M.S. and H.L. developed the laser structure. J.W., M.T. and H.L. performed material growth. S.C. and Q.J. carried out the device fabrication and device characterization. S.S., S.N.E. and P.M.S. performed laser near-field measurements and analysis. A.S. and S.S. contributed to the development of device processing. W.L. and I.R. performed TEM characterization and analysis. M.T. and J.W. carried out AFM characterization. S.C., J.W., A.J.S. and H.L. composed the manuscript with input from all co-authors.

Additional information

Supplementary information is available in the online version of the paper. Reprints and permissions information is available online at www.nature.com/reprints. Correspondence and requests for materials should be addressed to S.C. and H.L.

Competing financial interests

The authors declare no competing financial interests.

Methods

Crystal growth. The epitaxial materials were fabricated using a solid-source Veeco Gen-930 molecular beam epitaxy system. Phosphorus-doped Si(100) wafer with a 4° offcut to the [011] plane was used. Before material growth, oxide desorption of silicon substrates was performed at 900 °C for 30 min. Epitaxy was then performed in the following order: a 6 nm AlAs nucleation layer, a 1 μm GaAs buffer layer, InGaAs/GaAs dislocation filter layers, and five layers of InAs/GaAs DWELL structures separated by 50 nm GaAs spacers in the middle of a 140 nm undoped GaAs waveguide between 1.4 μm n-type lower and p-type upper $Al_{0.4}Ga_{0.6}As$ cladding layers. Each DWELL structure consisted of a three-monolayer layer of InAs QDs sandwiched by 2 nm $In_{0.15}Ga_{0.85}As$ and 6 nm $In_{0.15}Ga_{0.85}As$. The DWELLs were grown at 510 °C and GaAs and AlGaAs layers at 590 °C. Finally, a 300 nm p-type GaAs contact layer was grown.

Device fabrication. The broad-area lasers with 50-μm-wide stripes were fabricated by standard lithography and wet chemical etching techniques, and the ridge was etched to about 100 nm above the active region, to give improved carrier confinement. Ti/Pt/Au and Ni/GeAu/Ni/Au were deposited on the p^+-GaAs contact layer and exposed n^+-GaAs buffer layer to form the p- and n-contacts, respectively. After lapping the silicon substrate to 120 μm, the lasers were cleaved to the desired cavity lengths and mounted (as-cleaved) onto the heatsink.

Measurements. AFM measurements were performed with a Nanoscope Dimension 3100 SPM AFM system under ambient conditions using a non-contact mode. Conventional scanning TEM was performed using a JEOL 2010F field-emission gun TEM operating at 200 kV. Dislocation density measurements were derived from a series of bright-field scanning TEM images using a conventional inset-grid method and electron energy-loss spectroscopy to calculate the sample thickness. High-resolution high-angle annular dark-field Z-contrast scanning TEM images were acquired with a JEOL R005 aberration-corrected TEM operating at 300 kV with a convergence semi-angle of 21 mrad and a TEM inner annular collection angle of 62 mrad. The reliability study was carried out in auto current control (ACC) mode at 26 °C under a constant c.w. current stress of 210 mA. The output power was collected from a photodetector normal to the laser facet, while periodic LIV measurements were taken to monitor the changes in lasing threshold. Other standard laser device characteristics were all measured under c.w. and pulsed conditions (1% duty cycle and 1 μs pulse width).